

Viscoelastic Behavior of Flexible Slabstock Polyurethane Foams: Dependence on Temperature and Relative Humidity. I. Tensile and Compression Stress (Load) Relaxation

J. C. MORELAND,¹ G. L. WILKES,^{1,*} and R. B. TURNER²

¹Department of Chemical Engineering and Polymer Materials and Interfaces Laboratory, Virginia Polytechnic Institute and State University, Blacksburg, Virginia 24061-0211, and ²Polyurethanes Products Research, Dow Chemical Company, Freeport, Texas 77541

SYNOPSIS

The relaxation behavior of the load in compression and the stress in tension was monitored at constant temperature and/or relative humidity for a set of four slabstock foams with varying hard-segment content as well as two of the compression molded plaques of these foams. The majority of the compression relaxation tests were done at a 65% strain level in order to be consistent with the common ILD test. The tensile stress relaxation tests were performed at a 25% strain level. Over the 3-h testing period, a linear relationship between the log of compressive load or the log of tensile stress versus log time is observed for most testing conditions. For linear behavior, the values of the slope or the load/stress decay rate are comparable in both the tension and compression modes with the values being slightly higher in magnitude for the compression mode. These rates of decay are in the range of -2.2×10^{-2} to -1.7×10^{-2} for a 21 wt % hard-segment foam and -3.2×10^{-2} to -2.4×10^{-2} for a 34 wt % hard-segment foam. Increasing %RH at a given temperature does bring about a steady decrease in the initial load or initial stress as well as a slight increase in the rate of relaxation. The effect of temperature on the relaxation behavior is most significant at temperatures near 125°C and above. The FTIR thermal analysis of the plaques indicates that this significant increase is due to additional hydrogen bond disruption and possible chain scission taking place in the urea and urethane linkages that are principally present in the hard segment regions. The relaxation behavior in both tension and compression is believed to be mostly independent of the cellular texture of the foam at the strain levels given above. This conclusion is based on the similar relaxation behavior between the plaques and the foams. © 1994 John Wiley & Sons, Inc.

INTRODUCTION

The viscoelastic behavior in flexible polyurethane foams is of importance due to its relationship to the recoverability in the foam's shape and behavior after it has been compressed or fatigued. This behavior has been generally characterized by ASTM tests which mimic the application of these materials. Thus, these tests are normally carried out in compression and include such tests as compression set as well as static and dynamic fatigue.¹⁻⁷ Also,

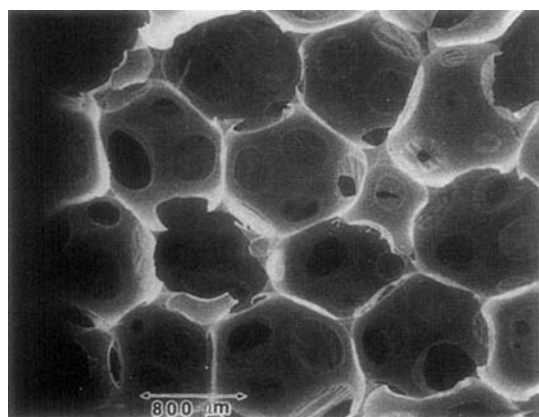
the viscoelastic behavior described by these tests in polyurethane foams have been shown to be a function of the environmental conditions and to depend on the foam formulation. Therefore, in order to further understand the viscoelastic behavior of flexible polyurethane foams, stress relaxation and creep measurements under controlled conditions of temperature and relative humidity have been made on a series of variable hard-segment flexible water-blown foams as well as the compression molded plaques of these same foams. Stress relaxation and creep are commonly utilized to characterize the viscoelastic behavior of polymeric materials by measuring the stress decay or change in strain with time at a constant strain or load, respectively. Thus, these

* To whom correspondence should be addressed.

tests enable one to be able to monitor the changes that are taking place with time during compression set or static fatigue tests. Also, of importance in characterizing the viscoelastic behavior of flexible foams is to have an understanding of the morphology, both macroscopic and microscopic. It so happens that the work presented in this paper is on the same series of foams utilized in recent morphological studies. Thus, before reviewing previous viscoelastic measurements on flexible polyurethane foams, mainly those of compression set, a brief overview of the morphology of the foams used in this present study is given.

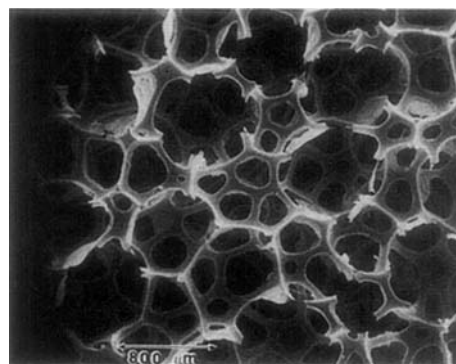
In the previous studies, a systematic series of four slabstock foams which varied in hard-segment con-

tent (21–34 wt %) were characterized by using several different morphological and structural techniques.^{8–10} In addition, the thermal compression-molded plaques of these foams were also studied in order to analyze the material comprising the foam *independent of its cellular geometry*. The general cellular morphology of these foams is presented in Figure 1—looking both perpendicular and parallel to the blow direction and thus showing the anisotropy of the cells for these materials. This distinct anisotropy is of importance especially when characterizing the mechanical properties of foams and does result in higher stress levels upon either compressing or stretching the foam parallel to the blow axis. However, its effect on the viscoelastic properties of



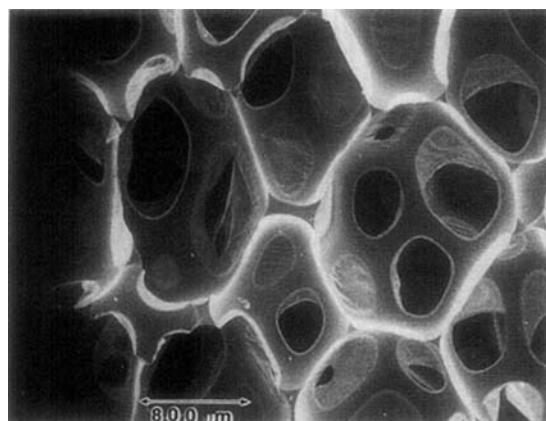
PARALLEL

(a)

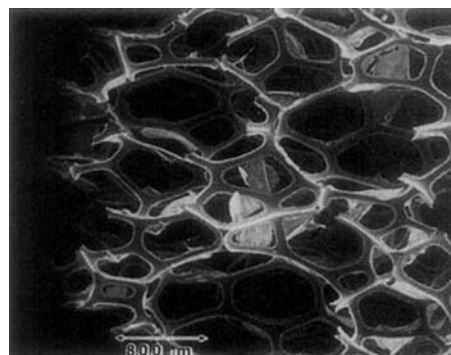


(b)

PARALLEL



PERPENDICULAR



PERPENDICULAR

Figure 1 SEM micrographs of foams F1 (a) and F4 (b). Observation direction is parallel (top) and perpendicular (bottom to the blow direction).

flexible foams is not known and thus will be addressed within this paper. One of the main reasons behind carrying out these morphological and structure-property studies, was to better understand the morphology of the solid portion of the foam or in other words the struts and the cellular wall material seen in Figure 1. While, the results from the different techniques could be summarized here, only the latest proposed schematic model based on the results from these techniques is given in Figure 2. The interested reader is referred to references 8–10 for further detail. As shown in Figure 2, a fairly well phase-separated system exists similar to that of urethane and urea-urethane elastomers. The larger structures specified as “polyurea” represent the urea-based aggregates which were thought to be of a reinforcing nature within the system. Also represented in Figure 2 are the smaller hard domains which should not be confused with the larger aggregate structures. The smaller hard domains are believed to be rather typical in size of those that exist in urea-urethane and urethane elastomers of comparable hard-segment content. An important difference, however, from that of the elastomers is the presence of a covalent

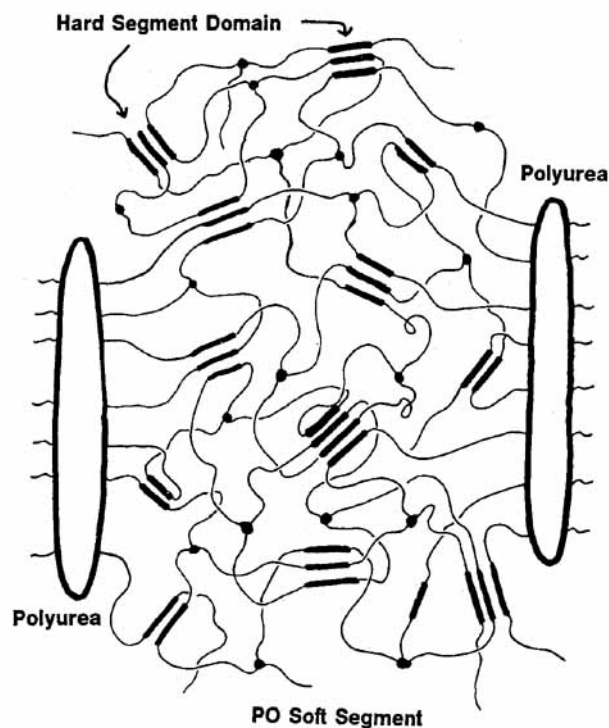


Figure 2 Schematic morphological model for the solid portion of the flexible slabstock polyurethane foam. The polyurea aggregates are shown as lamella-like particles, whereas the hard-segment domains are less lamella like and would be of considerably smaller size than the polyurea aggregates (not shown to scale). (From Ref. 10).

network in the foams promoted by the soft-segment glycerin extended polypropylene oxide units. This, of course, will have an influence on the long-term creep, stress relaxation, and level of extensibility as will be demonstrated to some extent in this article.

As mentioned above, compression set is one of the common properties measured to characterize the viscoelastic nature of flexible polyurethane foams. Compression set is basically a measure of the recovery of the foam height after subjecting a foam to a constant deflection at a given set of conditions [usually 23°C–50% relative humidity (RH)] for an extended period of time (usually 22 h). Several authors have measured the compression set in slabstock foams and more so in high-resilient (HR) foams.^{1–5} Most of these studies have concentrated on the effects of formulation variables as well as temperature and relative humidity effects on compression set. The water content has shown the largest effect on compression set, especially under humid conditions.^{1–3} Herrington and Klarfeld, for example, reported humid aged compression set (HASET) values increasing with water content, that is, urea content, after exposing the foams for 5 h of 121°C and 100% RH conditions and then a 50% deflection for 22 h at the usual compression set conditions.² Patten and Seefried also observed the same trend for 50% HASET values under similar testing conditions.¹ In addition, Saotome et al. reported a more significant increase in compression set with increasing water content for compression set tests that were carried out *under conditions* of 50°C and 95% RH for 22 h.³ The above results indicate that the urea content or the hard-segment content has a significant effect on the humid aged compression set. A more detailed explanation is given in the next paragraph.

Herrington and Klarfeld also reported on the effects of temperature and relative humidity from their compression set study of HR foams. These authors observed lower 50% HASET values upon humid aging at 104°C rather than at 121°C as well as by exposing the foams to low humidity versus high humidity at 121°C.² In addition, the change in the 50% HASET values were almost negligible with increasing water content at the lower temperature and there were no changes with water content at the lower humidity. These results indicate that both temperature and humidity are affecting the recovery of the foam's thickness. In the case of relative humidity, it has been suggested by several authors that water acts as a plasticizer thereby allowing for more chain slippage to occur.^{2,4,6} Along these lines, Herrington and Klarfeld proposed a model that suggested that

hydrogen bonds to the urea carbonyls of the hard segments are replaced by water molecules during humid aging. Upon compressing the foam, many of the water to water hydrogen bonds are broken which allows for chain slippage to occur. Thus, in the compressed state, a new equilibrium takes place, and, upon release, a rather significant loss in the foams thickness results.²

In a different study, Lee measured the compression set and the hysteresis loss, that is, the energy loss during the compression set for an HR flexible foam.¹¹ Lee concluded from his tests that the compression set depends heavily on the hysteresis loss. Dwyer also observed that the %ILD loss was also related to the hysteresis loss.¹² The authors of these studies attributed the hysteresis to the large amount of stress relaxation that takes place during the prolonged compression (22 h).

The above reports from the literature do provide information on how the formulation components as well as the surrounding conditions effect the recoverability of the shape and strength of flexible foam. However, the reports in the literature have not focused on the actual viscoelastic behavior, that is the stress relaxation behavior or in other words the change in stress over time while under a constant strain level. In addition, the effects of temperature and relative humidity on this behavior during deformation have not been examined thoroughly as well as over a wide range of controlled conditions. Also, the effect of the foam's cellular texture on the viscoelastic behavior has not been reported on in the literature. In addressing these points, the effects of temperature and relative humidity on the stress relaxation behavior in tension and compression are presented in this paper for a systematic series of

foams that were mentioned above. It is also important to note that while the tensile stress relaxation test is not "applications oriented" toward polyurethane foams, it does offer the ability to easily probe the struts and the cellular wall material. In addition, it allows direct comparison to the solid plaques of the foams which cannot be easily studied in the compressive mode.

EXPERIMENTAL

The foams utilized in this work were a series of variable hard-segment content flexible slabstock foams used and described in earlier studies (mentioned above).⁸⁻¹⁰ The nomenclature as well as the composition variables and density of these foams are summarized in Table I. The formulation components used to produce these foams were a 80 : 20 mixture of 2,4 and 2,6 isomers of toluene diisocyanate, TDI (T-80, DOW) 3000 MW polypropylene oxide-glycerine initiated polyol (DOW), water, silicone surfactant Goldschmidt, as well as tin and amine catalysts. As shown in Table I, isocyanate and water content levels have only been adjusted while keeping other component levels constant. The two main foams used in this work were foam F1 and foam F4 which consist of the extremes in composition for this series (see Table I). The compression-molded plaques of foams F1 and F4 were also utilized in this study. These plaques are referred to as P1 and P4 and were made by compressing their respective foam at 204°C for 10 min. Note that plaques P1 and P4 offer the advantage of being able to study the foams independent of the cellular geometry since the morphological features of the solid portion of the foam and its plaque are believed to be rather similar based

Table I Compositional and Physical Parameters of Foams F1-F4 and Plaques P1 and P4

Materials				
Foam/Plaque	pph H ₂ O	pph TDI	Density (lb/ft ³)	wt % HS
F1	2	30.79	2.85	21.1
F2	3	41.43	1.92	25.8
F3	4	52.06	1.43	30.1
F4	5	62.70	1.24	33.8
P1	2	30.79	—	21.1
P4	5	62.70	—	33.8

Note: A 3000-MW glycerine initiated poly(propylene oxide) polyol was used. Formulations based on 100 parts by weight of polyol. All other component levels were held constant; 110 TDI index. Plaques were compression molded from foams F1-F4 at 204°C for 10 min.

on earlier studies.⁹ In addition to studying the foams and the plaques, we also utilized a chemically similar polyurea-urethane (PUU) elastomer that had no covalent network structure for comparison purposes to the foams since the foams are also urea-urethane materials. The formulation components were T-80, 2000 MW PO diol, and methylene-bis(2-chloroaniline) MOCA chain extender. The elastomer was prepared at Dow Chemical by utilizing a two-step reaction with 5% extra NCO groups. The resulting elastomer contained a 31 wt % hard-segment. Its films were cast from a DMF solution which was followed by a thorough drying process.

The controlled temperature tensile stress relaxation experiments were carried out on a Tensilon tensile tester equipped with a 550-g load cell and a homemade thermal chamber. The controlled humidity-temperature tests were done using an MTS tensile tester equipped with the same load cell and a Thermitron environmental chamber. The variable temperature studies were done at 25, 50, 75, 100, 125, and 140°C. The controlled humidity test were carried out at temperatures of 30, 60, and 90°C with %RH levels at either low (2–15%), 50%, or high (95–100%). Dogbone samples cut from the ambient temperature stored foams with a 10-mm gauge length and 5 mm in thickness were used for both setups. Dogbone samples with a 10-mm gauge length were used for the plaques which were 5–8 mm in thickness as well as for the PUU elastomer which were 2–4 mm in thickness. These latter samples were only for the controlled temperature experiments. After mounting the samples in the clamps, the appropriate conditions were obtained and then maintained for 30 min before stretching the samples to a constant elongation of 25% at a 40 mm/min strain rate. The stress relaxation behavior was monitored by a computer over a 3-h time period. The experiment was repeated in the case of the controlled temperature tests three to four times on fresh samples. In the case of the controlled temperature and relative humidity tests for foams F1 and F4, the experiments were not repeated at all conditions, but were found to be quite reproducible at those conditions where additional tests were performed.

The experimental procedures followed for the compression load relaxation studies were not standardized tests given by ASTM standards for flexible foams.¹³ However, these experiments were developed based on the review of the literature and the need for a better understanding of the relaxation behavior as a function of time for flexible foams.¹⁴ The compression load relaxation tests were carried out on an Model 1122 Instron equipped with a 10-lb.

compression load cell as shown schematically in Figure 3. The conditions of the test were controlled by a Russells Technical Products environmental chamber (see Figure 3). The testing conditions ranged from 30 to 140°C (lowest possible RH) for the variable temperature tests. The effect of humidity was determined by varying the relative humidity from low (0–15%) to intermediate ($50 \pm 3\%$) to high (95–100%) at each of the temperatures of 30, 60, and 85°C. The foam samples used were 4" × 4" and were approximately 1" in thickness. They were cut so that they would be compressed parallel to the blow direction. A typical test involved placing a foam sample on the testing plate (5" × 5") and lowering a 2" diameter indenter so that it just touched the top of foam (see Fig. 3). The desired testing conditions were allowed to reach equilibrium and then were maintained for 30–45 min. At this point, the sample was compressed twice at a 350 mm/min cross-head speed in cyclic fashion to a 70% strain level to mimic the indentation load deflection (ILD) tests given in the ASTM procedural standards for flexible foams. At 5 min later the foam was compressed at the same cross-head speed to a constant strain level that was usually 65%. Upon reaching the constant strain level, the load was monitored periodically for 3 h and stored on computer (see Fig. 3). At most testing conditions, only one sample was used to measure the relaxation behavior. However,

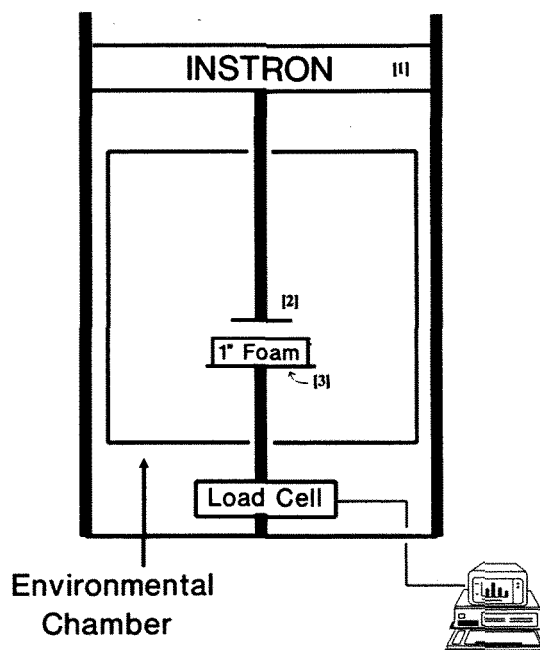


Figure 3 Experimental setup for compression load relaxation tests.

for some experimental conditions two or three samples for a given foam were tested to obtain a range of error in the measurements.

The effect of temperature on the foams was also carried out by analyzing the thermally compression-molded plaques with a Nicolet 5DXB FTIR spectrometer equipped with a homemade thermal chamber. This evaluation was done to determine the extent of hydrogen bond disruption with increasing temperature and furthermore to determine if any chain scission was taking place. The hydrogen bonding changes were evaluated by analyzing the IR spectra in the (N—H)-bonded (3300 cm^{-1} , C=O)-urea/bonded (1640 cm^{-1}), and the (C=O)-urethane ($1700\text{--}1730\text{ cm}^{-1}$) regions. The chemical degradation was evaluated through monitoring the free isocyanate band at 2270 cm^{-1} . From a qualitative standpoint, peak areas were measured for the (C=O)-urea/bonded, and peak heights were obtained for the other bands. In the latter case, peak heights were utilized due to band overlap in these areas of the spectra.

Within this paper, results obtained for the free isocyanate band will only be shown due to the high absorbance levels that were obtained for the other bands (> 0.7 or greater than the detector limits). However, the authors do believe that the results obtained in their analysis for the bands related to hydrogen bonding are reproducible as well as consistent with other findings from investigators of polyurethane and polyurethane materials. Thus, comments from these results will only be made and the interested reader is referred to reference 14 for further details.

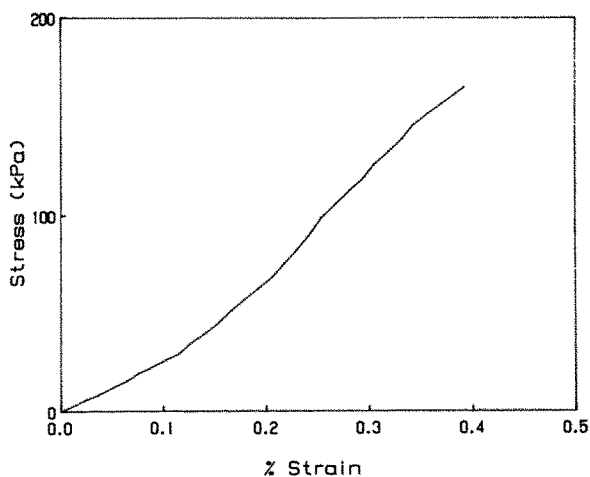


Figure 4 Tensile stress-strain curve for foam F4 (40 mm/min initial extension rate).

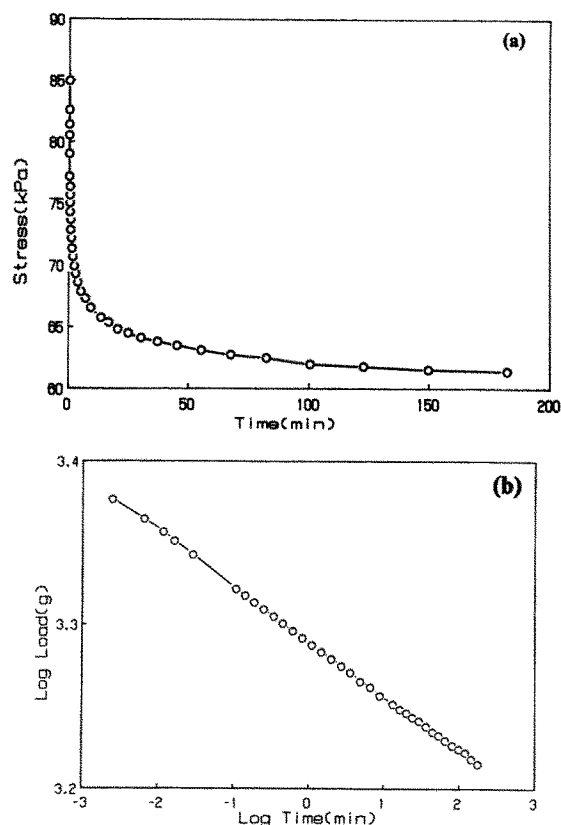


Figure 5 Stress relaxation behavior of foam F4 in tension at 25% elongation (a) linear stress versus linear time and (b) log stress versus log time.

RESULTS AND DISCUSSION

Tensile Stress Relaxation Behavior

In Figure 4, the typical stress strain profile for foams F1–F4 that was obtained at ambient conditions is displayed. As expected, there is very little curvature for the stress-strain behavior for these flexible foams.^{15,16} The stress relaxation behavior for foams F1–F4 was obtained by stretching the samples parallel to the blow direction to a constant strain level of 25%. The samples were only elongated parallel to the blow direction since earlier studies have shown similar relaxation behavior upon stretching the foams parallel and perpendicular to the stretch direction.¹⁷ This previous result also suggested that the viscoelastic behavior in tension is independent of the cellular texture of the foam and this point will be addressed further in later discussion. Before discussing the effects of temperature and relative humidity on the relaxation behavior in tension, the general relaxation behavior is shown at a 25% strain level for F4 in Figure 5. In Figure 5(a), the decay

of the stress is seen over time and in Figure 5(b), the decay of the log stress with log time is displayed. As shown in Figure 5(b), there is rather linear behavior for the $\log \sigma(t)$ versus log time. This type of behavior is observed at most conditions as will be shown below. Although, this particular relationship between stress and time has no molecular basis, it does provide a means of obtaining a stress decay rate (σ_d) by calculating the slope over the 3-h time period using linear least squares. Similar behavior for $\log \sigma(t)$ versus log time has also been observed for other polyurethanes as well as for other cross-linked polymeric materials.¹⁸⁻²¹

Effect of Temperature on Tensile Stress Relaxation Behavior

For the constant temperature tests in the range of 25–140°C, the relative humidity was not controlled due to the testing chamber that was utilized. While obtaining this data, the relative humidity was approximately 50% at 25°C and decreased as temperature was increased. The effect of relative humidity, however, in conjunction with temperature on the tensile stress relaxation behavior will be later addressed.

The $\log \sigma(t) - \log t$ variable temperature stress relaxation behavior is displayed as a three-dimensional surface in Figure 6 for the lower hard-segment foam, F1. The surface in Figure 6 was generated by applying a three-dimensional grid conversion developed by Cohort Software to the $\log \sigma(t) - \log t$ data obtained at various temperatures. As shown, the initial and 3-h stress levels go through a maximum with temperature at 100°C. The increase in the stress level up to 100°C is believed to be rather consistent with the theory of rubber elasticity which

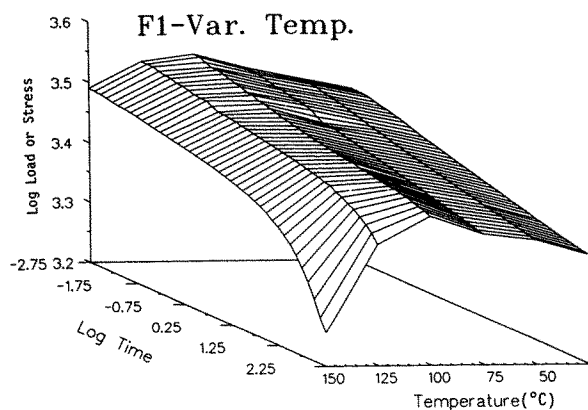


Figure 6 $\log \sigma(t) - \log t$ variable temperature stress relaxation behavior for foam F1.

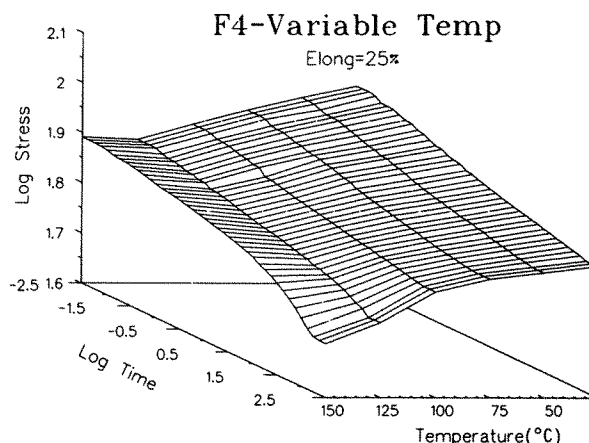


Figure 7 $\log \sigma(t) - \log t$ variable temperature stress relaxation behavior for foam F4.

predicts an increase in the level of stress with temperature at “equilibrium” conditions. In confirming this hypothesis, “equilibrium” stress values were calculated from the 3-h stress level at 25°C and compared to the values that were obtained experimentally. As displayed in Table II, a small negative deviation from predictions obtained by rubber elasticity exists up to 100°C which is not surprising since true equilibrium is not manifested in the results. Furthermore and more importantly, classical theory is not expected to directly apply to these microphase-separated systems, even though they do contain a covalent network structure through the glycerine-extended propylene oxide soft segment. Thus, the small deviations are thought to be mostly related to disruption and reformation of secondary bonding. This type of disruption has been indicated through FTIR thermal analysis which showed a steady decrease in the absorbance levels of the (N—H)-bonded and the (C=O)-urea bonded vibrations with increasing temperature. It could not be determined from the analysis if the hydrogen bond disruption was taken place mostly in the urea segments or the urethane segments due to (1) difficulty in quantifying the urea carbonyl vibrations between 1700 to 1740 cm^{-1} and (2) the unknown temperature dependence absorptivity coefficient for the (N—H)-bonded vibration. However, it was clear that with increasing temperature there was a consistent increase in the hydrogen bond disruption.

The variable temperature stress relaxation behavior for $\log \sigma(t)$ versus $\log t$ is shown in Figure 7 for the highest hard-segment containing material, foam F4. As shown in Table II, the initial stress levels are higher in F4 in comparison to those of F1. In addition, the initial stress level as well as the

3-h stress level decreases with increasing temperature for F4. This decrease in the stress levels and, in particular, the three-stress level is not consistent with rubber elasticity theory as shown in Table II. As stated above, this theory does not account for changes in secondary bonding which are thought to be fairly significant in F4 (at least in comparison to F1). Thus, it is believed that the disruption and reformation of hydrogen bonding in F4 is strongly contributing to the decrease in the initial as well as the final stress levels with increasing temperature.

For both foams F1 and F4, there is rather linear behavior for $\log \sigma(t) - \log t$ up to 100°C and thereafter there is nonlinear behavior (see Figs. 6 and 7). The values for the slope or stress decay rates, σ_d , are given in Table II for both foams. The rates of decay do decrease slightly with increasing temperature up to 100°C for F1 and F4. Also shown in Table II are the percent stress decay values which decrease slightly from 25 to 100°C and then begin to increase with temperature thereafter.

The values for the stress decay rates and the percent stress decay values within the temperature range of 25–100°C indicate that stress relaxation is approaching equilibrium conditions faster with increasing temperature for both F1 and F4. Several factors are thought to contribute to this acceleration of stress relaxation with increasing temperature. First, the relative humidity has not been controlled for these tests and it is believed that the humidity level as well as the effect of humidity on the stress relaxation behavior decreases with increasing temperature. Recall that the relative humidity was approximately 50% at ambient conditions ca. 25°C. Another factor is the amount of stress relaxation that takes place while reaching the constant strain level, this is thought to increase with temperature. This increase can be attributed to several processes. One thermally activated process is that soft segments relax much faster or are on a shorter time scale due to more mobility in their chains. Another mechanism is hydrogen bond disruption which leads to chain slippage between molecular chains including the hard-segment units. This type of disruption is most likely a result of a weakening of hydrogen bonds with increasing temperature which has been supported by the FTIR-thermal study of the compression molded plaques of foams F1 and F4.¹⁴

At temperatures greater than 100°C, a more significant increase in the amount of stress relaxation is observed in foams F1 and F4 as shown in Figures 6 and 7, respectively as well as in Table II for both foams. This increase is indicated by the higher percent of stress decay values and the nonlinear be-

havior in the $\log \sigma(t)$ versus the $\log t$ plots for F1 and F4. One reason for these more rapid changes in the stress relaxation rate at higher temperatures is due to an increase in the disruption of hydrogen bonds with increasing temperature that has been indicated by the FTIR-thermal behavior for plaques P1 and P4.¹⁴ Another reason suggested by the FTIR-thermal studies, is possible chain scission that is thought to be taking place in the urethane and urea linkages. In Figures 8(a and b), support for possible chain scission in foams F1 and F4 is given by the observation of free isocyanate (ca. 2275 cm^{-1}) at temperatures greater than 100°C. Both of these changes, that is, hydrogen bond disruption and chemical degradation in the structure of the foam will lead to further local chain slippage, which, in turn, causes more stress relaxation to occur.

Some additional comments are necessary when comparing the stress relaxation behavior of foams F1 and F4. As shown in Figure 9, the amount of stress relaxation as a function of temperature is higher for foam F4 than for foam F1, except at

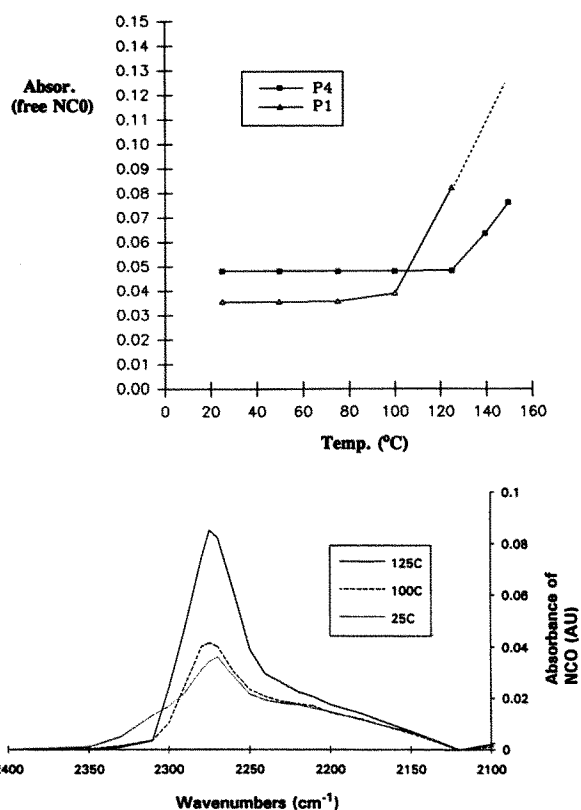


Figure 8 (A) Free isocyanate region of FTIR spectrum for plaque—as a function of temperature for plaques P1 and P4. (B) Absorbance of free isocyanate as a function of temperature for plaques made from foams F1 and F4.

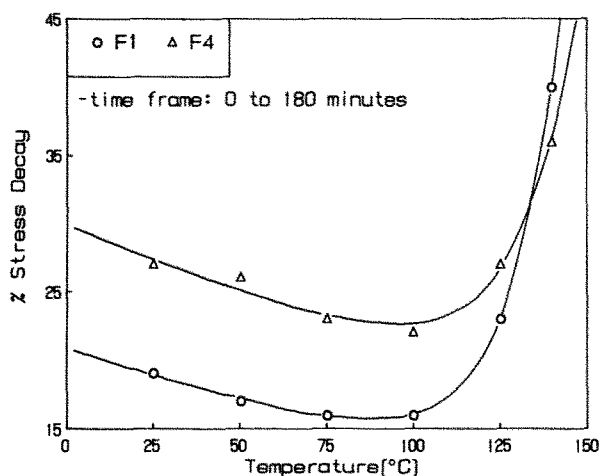


Figure 9 Percent stress decay at different temperatures for foams F1 and F4 (data points have been fitted by eq. (1)).

140°C. Also, the stress decay rates are higher in magnitude for foam F4 than F1 at a given temperature (see Table II). Finally, the negative deviation from rubber elasticity predictions increase systematically with increasing temperature for both foams F1 and F4, but to a greater extent for F4. Most of these differences can be related to the higher hard-segment content of foam F4 and thus more available hydrogen bonds to undergo disruption. On the other hand, the behavior at 140°C suggests that additional mechanisms for stress relaxation are taking place in foam F1 and certainly in foam F4 as well (see Figure 9). As mentioned above, the FTIR-thermal studies for the plaques of these foams, indicated that additional hydrogen bond disruption to the urea and urethane groups is believed to occur thereby softening the hard-segment interactions. Furthermore, chain scission is also speculated to be taking place in the urethane linkages as well as in the urea linkages. In addition, based on the results from the FTIR thermal analysis shown in Figure 8, these structural changes are believed to be greater in foam F1 in comparison to foam F4; thus giving reason for the larger amount of relaxation observed at 140°C for F1. Greater changes at the higher temperatures are likely to occur in F1 since it is believed to have a lower structural order and less hydrogen bonding to the urea hard segments in comparison to the higher hard-segment foam, F4.

In further evaluating the stress relaxation behavior for foams F1 and F4, the results given in Figure 9 for the thermal dependence of stress decay have been fit using a two-parameter model. As shown in Figure 9, there are two distinct portions of the

response for foams F1 and F4. Thus, one requirement of the model is to account for the slight decrease in the stress decay values up to 100°C. The second is to account for the significant increase in the amount of stress relaxation at temperatures greater than 100°C. This two-parameter model, though empirical, does somewhat resemble a generalized two component Maxwell-Wiechert model, and is as follows:

Stress Decay

$$= C_1 \exp \left[\frac{-T}{\tau_1} \right] + C_2 \exp \left[\frac{T - T_0}{\tau_2} \right] \quad (1)$$

where C_1 and C_2 are constants (front factors), τ_1 and τ_2 are temperature relaxation constants with units of reciprocal °C, and T_0 (°C) is a constant which takes on a value (ca. 100°C) near the up-turn in the stress decay-temperature behavior (see Figure 9). The constants in eq. (1) were obtained by setting T_0 and C_1 to constant values and letting a BASIC program designed by R. W. Ramette of Carleton College obtain the best fit for the data by changing the other variables. As shown in Figure 9, the two-parameter model fits the data very well and does account for the two different parts of the curve. Also, the temperature relaxation constant, τ_1 , for F4 ($\tau_1 = 252$) is slightly lower than τ_1 for F1 ($\tau_1 = 258$). This small difference indicates that increasing temperature in the range of 25–100°C results in a somewhat greater acceleration of the stress relaxation process for F4 in comparison to that of F1. On the other hand, τ_2 is greater for F1 (14.9) than F4 (18.3), which signifies a more significant thermal effect on the stress relaxation of foam F1 at the highest temperatures. Further utility of this empirical model will be demonstrated later within this paper.

As mentioned earlier, the compression-molded plaques of the foams were also utilized to characterize the relaxation behavior of the solid portion of the foam independent of its cellular geometry. Recall, for example, that P1 is compression molded from foam F1. In Figure 10, the variable temperature $\log \sigma(t) - \log t$ relaxation behavior for P1 is shown in the three-dimensional form. As noted, the initial stress level increases very systematically with increasing temperature and as in the case of F1, the 3-h stress level goes through a maximum near 100°C (compare Figs. 6 and 10). The stress relaxation behavior is nearly linear for the $\log \sigma(t)$ versus $\log t$ plots up to 100°C and thereafter exhibits nonlinear behavior. For the "linear" behavior, the stress decay rates for P1 are analogous to those of F1 as given

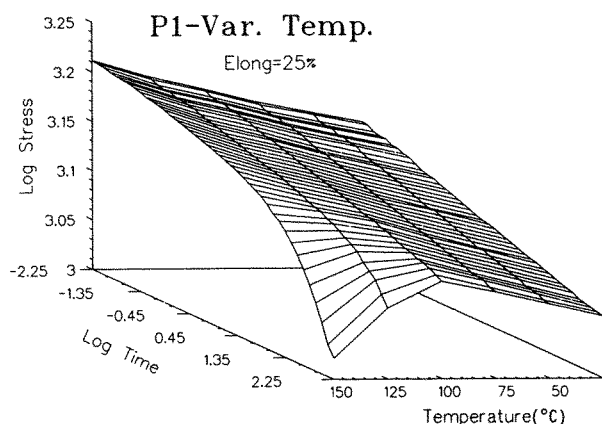


Figure 10 $\text{Log } \sigma(t) - \text{Log } t$ variable temperature stress relaxation behavior for plaque P1.

in Tables II and III, respectively. In addition, as shown in Figure 11 the stress decay values as a function of temperature are very similar for F1 and P1. Also shown in Figure 11 is very comparable behavior between the stress decay values for F4 and its respective plaque, P4. Although, the stress relaxation behavior is not shown here for P4, it has many similarities to that of F4 as well (compare Tables II and III). *In short, the similar behavior in Figure 11 gives further indication that the stress relaxation behavior is independent of cellular texture and thus is dependent on the solid portion of the foam.*

In further evaluating the effect of temperature on the stress relaxation behavior for microphase-separated segmented materials, the PUU thermoplastic elastomer was utilized. It is recalled that the PUU elastomer was made with many chemically similar components to those used in preparing the foams. However, the noteworthy point is that the *linear* TPU elastomer has a segmented morphology, whereas the foams also possess a covalent network structure in addition to a two-phase hard/soft domain texture with large urea aggregates.

The $\text{log } \sigma(t) - \text{log } t$ stress relaxation behavior at temperatures ranging from 25 to 125°C is shown for the PUU elastomer in Figure 12 as determined at a constant elongation of 25%. The stress decay rates along with the initial stress levels and percent stress decay values are given in Table IV. As shown in Figure 11, the behavior again is rather linear up to temperatures of 100°C and then begins to exhibit negative deviation at 125°C. The linear behavior is quite similar to that displayed earlier in Figures 5 and 6 for foams F1 and F4. However, there is a more significant increase in the amount of stress relaxation taking place from 100 to 125°C for the PUU elastomer than in the case for F1 and F4 (see Tables II and IV). A similar transition in the same temperature region has also been reported for stress relaxation results obtained at a 25% elongation for another segmented polyether polyurethane elasto-

Table II Summary of Results for Variable Temperature Stress Relaxation

Temperature (°C)	Initial Stress ^a (kPa)		% Stress Decay ^b		Slope ($\times 10^2$) ^{c,d}		% Deviation ^e	
	F1	F4	F1	F4	F1	F4	F1	F4
25	32	98	20	27	-2.2	-2.9	—	—
50	34	93	17	26	-1.8	-3.0	0	-11
75	35	88	16	23	-1.7	-2.6	-2	-19
100	37	83	16	22	-1.7	-2.4	-4	-26
125	36	77	23	27	-2.3	-2.9	-20	-42
140	32	78	40	36	-4.2	-3.9	-46	-50

^a Initial stress level obtained in ca. 0.3 s following elongation.

^b Time frame is from 0 to 180 min.

^c Slope is obtained by linear least squares of log stress-log time data points; correlation coefficient within 0.995–0.999 except at 125 and 140°C.

^d The reader should note that a linear least square regression analysis was also applied to the data obtained at the higher temperatures where clearly nonlinearity occurs. However, this calculated 3-h slope still provides a base of comparison with the lower temperature data which does behave quite linearly. Hence, as the comparisons are made, the reader should keep this in mind for certainly the higher temperature data at longer times is decaying even more rapidly than the linear regression analysis would indicate.

^e % Deviation from predictions given by rubber elasticity theory; predictions based on the stress level at 25°C and 180 min.

Table III Summary of Results for Variable Temperature Stress Relaxation for Plaques P1 and P4

Temperature (°C)	S_0 (MPa)		% Stress Decay ^a		Slope ($\times 10^2$) ^b	
	P1	P4	P1	P4	P1	P4
25	1.4	6.7	18	29	-2.0	-3.2
75	1.5	6.85	17	24	-1.9	-2.7
100	1.5	6.3	18	24	-1.9	-2.7
125	1.6	6.15	25	29	—	—
140	1.6	5.6	37	35	—	—

^a Time frame is from 0 to 180 min.
^b Correlation coefficient within 0.995–0.999 except at 125 and 140°C.

mer by Seymour et al.²² Based on the FTIR-thermal analysis of the PUU elastomer, this significant increase in the amount of stress relaxation for the PUU elastomer is attributed to the disruption of hydrogen bonds and to possible chain scission taking place in the urea and urethane linkages.¹⁴ This conclusion is also consistent with and gives support to the above arguments presented for the foams in explaining the large changes in the stress relaxation behavior at temperatures greater than 100°C. It is clearly noted that the rates of relaxation as well as the stress decay values are higher for the PUU elastomer in comparison to the foams (see Tables II and IV). This type of behavior is certainly expected since the elastomer has a linear segmented morphology, whereas the foams also possess a covalent

network. Also, these materials are chemically different since the PUU elastomer contains an MOCA chain extender, whereas the foams do not.

Effect of Relative Humidity on Tensile Stress Relaxation Behavior

As mentioned in the discussion for the variable temperature studies, the percent relative humidity was not controlled or monitored. Since humidity is known to effect the properties of flexible polyurethane foams, results are presented in this section from tests where both temperature and relative humidity have been controlled. Before discussing these results, it is of importance to have some idea of how water may interact with the foams and potentially how it might affect the physical properties of these materials. Some potential sites for water to interact to the chemical structure of the foam are ether linkage of the soft segment and the carbonyl and N—H

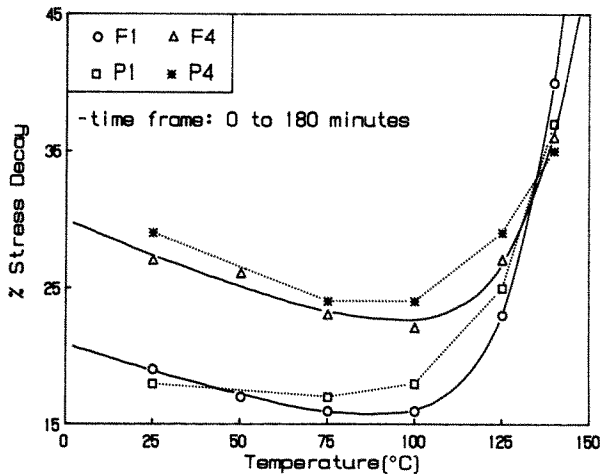


Figure 11 Percent stress decay at different temperatures for foams F1 and F4 and their respective plaques. The solid lines through the data for the foams were generated by the empirical model. The dotted lines through the data from the plaques have no particular significance.

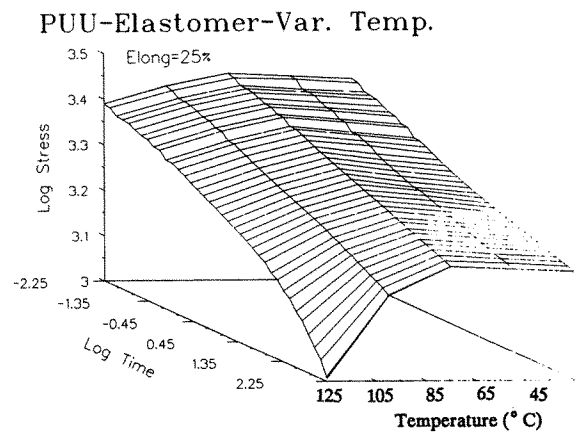


Figure 12 $\text{Log } \sigma(t) - \text{Log } t$ variable temperature stress relaxation behavior for PUU elastomer.

Table IV Variable Temperature Stress Relaxation Results for the PUU Elastomer

Temperature (°C)	σ_0 (MPa)	% Stress Decay	-Slope ($\times 10^2$) ^a
25	2.8	37	4.4
75	2.85	37	4.6
100	2.7	43	5.4
125	2.45	59	8.1

Note: Correlation coefficient was in the range of 0.995–0.999, except at 25 and 125°C.

groups on the urethane linkages (interface) and urea linkages (hard segment). At the molecular level water is thought to interact more with the hard segment due to more possible chemical sites and a greater affinity with these sites. On the other hand, for the chain structure (see Fig. 2), the extent of water interaction with the different morphological units (hard vs. soft) is not known, and, furthermore, it is not known how the extent of this interaction changes with temperature and relative humidity. In obtaining a better understanding of these unknown facts, some weight uptake measurements on the solid plaques of foams F1 and F4 were carried out at saturated conditions at 23°C and 38°C. It was also desired to quantify the weight uptake at higher temperatures, that is, 90°C, but due to experimental difficulties, this was not successful.¹⁴ The results obtained for the equilibrium weight uptake of water at 23°C for the plaques of foams F1 and F4 were the same. However, at 38°C, the percent weight uptake is higher for both plaques and was about 20% more higher for P4 than P1.¹⁴ This rather significant difference in weight uptake between the two plaques was somewhat expected since there are four times as many urea linkages available in F4 versus F1. As discussed above, the urea-based hard segments are thought to have a greater affinity for water than that of the soft segments. In an attempt to further answer the above questions on the affinity of water for these materials and how humidity effects the viscoelastic behavior, the stress relaxation results for F1 and F4, are now discussed.

The $\log \sigma(t) - \log t$ stress relaxation behavior at 30 and 90°C from low to high humidity is shown for foams F1 and F4 in Figures 13(a, b) and 14(a, b), respectively. The stress decay rates and the percent stress decay values at 30, 60, and 90°C are summarized in Table 5 for both foams F1 and F4. At these three temperatures, the stress level at a given time does decrease systematically with increasing relative humidity as shown in Figures 13 and 14. This behavior is consistent with reports in the literature for studies performed in compression under

controlled humidity and temperature.^{4,12} In addition, it also indicates that water is acting as a plasticizing agent by causing increased chain slippage.

Interestingly, the effect of humidity on the stress relaxation behavior is not that significant at 30 and 60°C for both F1 and F4 as indicated by the numbers in Table V. The change in the amount of stress decay for F1 (15%) is actually slightly greater than that of F4 (7%) at 30°C and about the same at 60°C. Thus, this indicates the effect of humidity on the

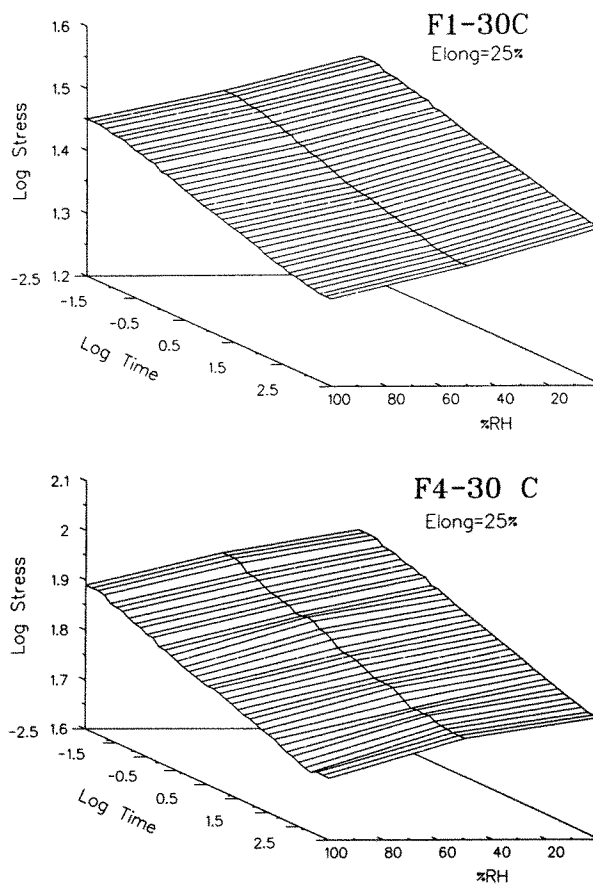


Figure 13 Effect on humidity on the stress relaxation behavior at 30°C for (a) F1 and (b) F4.

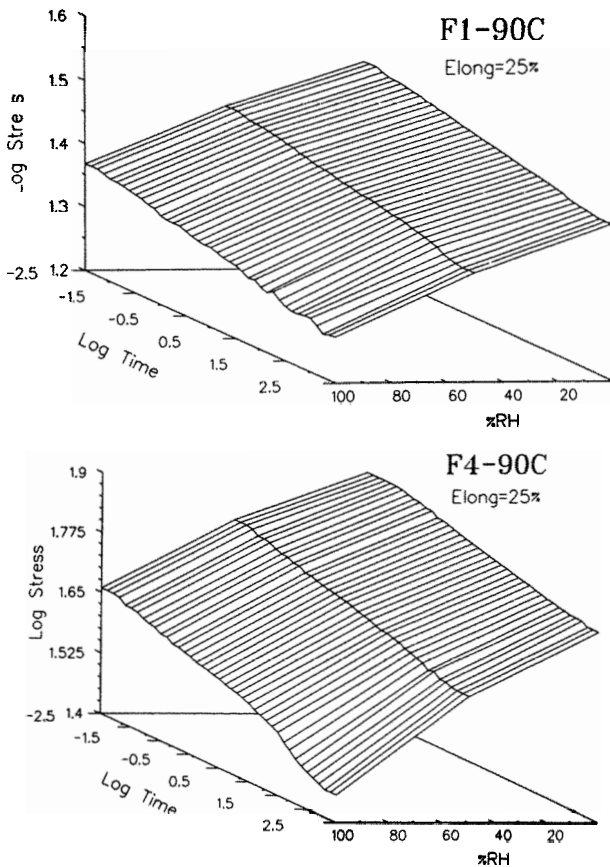


Figure 14 Effect on humidity on the stress relaxation behavior at 90°C for (a) F1 and (b) F4.

relaxation behavior at 30°C is greater for F1 than F4 and hence suggests that the interaction of water with F1 is greater than that for F4 at the lower temperature. At 90°C, the effect of humidity on the stress relaxation behavior is more significant for both foams F1 and F4 (see Table V and Figure 14). Interestingly, this effect is now greater for F4 than F1 as shown by comparing the response surfaces in

Figure 14. In addition, the change in the percent stress decay for F4 (54%) is higher than that of F1 (35%). These differences in the relaxation behavior at the higher temperature for both foams F1 and F4 indicate that water is interacting more with F4 due to its higher hard-segment content. It also appears from the change in the amount of relaxation occurring at 30 and 90°C that the weight uptake of water increases to a greater extent with temperature for F4 in comparison to F1. This trend is also consistent with the few results obtained from the weight-uptake studies at 23 and 38°C. One possible reason for this increased effect of humidity on the stress relaxation behavior of F4 at the higher temperatures, is that the ability of water to enter into the hard domains is more facilitated by the weakening of the hydrogen bonding with increasing temperature.

In summarizing the results for the effect of humidity as well as temperature (up to 90°C) on the tensile stress relaxation behavior for the 3-h time period, the three-dimensional response surfaces are shown in Figures 15 and 16 for foams F1 and F4, respectively. Both F1 as well as F4 show that as one increases temperature, the rate of relaxation for the most part is lower, except at the highest relative humidities and especially for F4 at 90°C. At low relative humidities, the thermal dependence of the stress decay rates indicate that the approach to an equilibrium stress level is faster and has been accelerated by increasing the temperature. However, this is not the case at the higher temperatures of 125 and 140°C as displayed in Figures 5 and 6. As shown there is rather nonlinear behavior at these higher temperatures and, furthermore, there is an increase in the amount of relaxation taking place over the 3-hour time period (see Table II). Finally, as shown in Figures 15 and 16, the effect of increasing relative humidity at 30 and 60°C is small, but is much greater at 90°C. Therefore, based on results presented and discussed for the stress relaxation be-

Table V Percent Stress Decay at Different Temperature-Humidity Conditions

Foam	Temperature (°C)	% RH =	% Stress Decay (from 0 to 180 min)		
			0.15	50	95-100
F1	30	20	21	22	
F4	30	30	31	32	
F1	60	20	22	23	
F4	60	28	29	32	
F1	90	17	19	23	
F4	90	24	28	37	

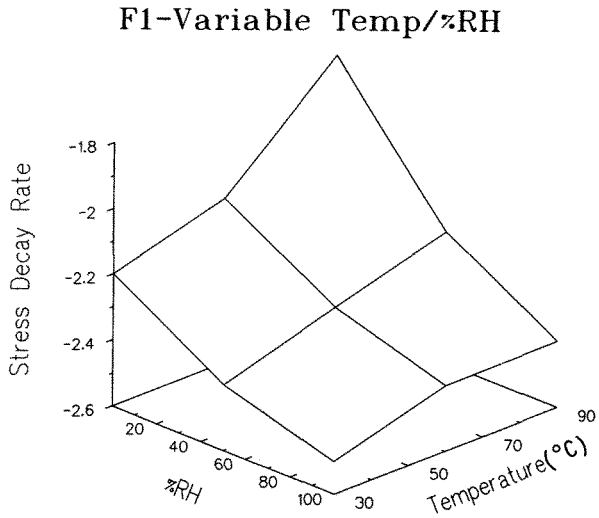


Figure 15 Effects of temperature and humidity on the stress relaxation behavior for F1.

havior of these materials, it is concluded that temperature has a more significant effect than relative humidity on the viscoelastic nature of flexible polyurethane foams. It is clear, however, that the humidity is also an important parameter. In continuation of the understanding of these effects as well as others on the viscoelastic behavior of flexible foams, results from a more applications-oriented test, that is, compression load relaxation, are presented below.

Compression Load Relaxation Behavior

The compressive load-strain behavior along with the different “regimes” for this behavior are presented

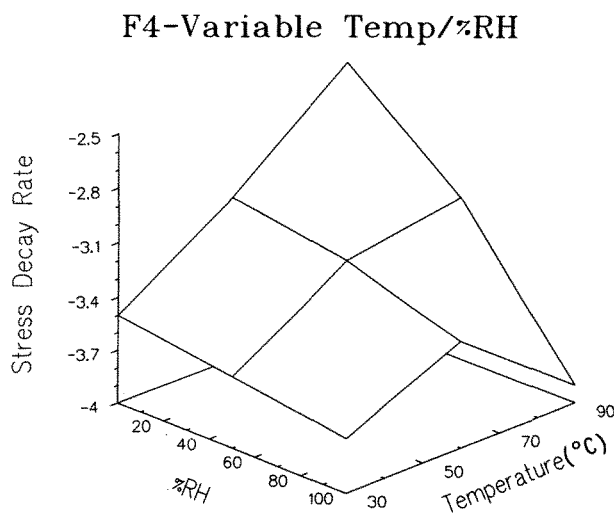


Figure 16 Effects of temperature and humidity on the stress relaxation behavior for F4.

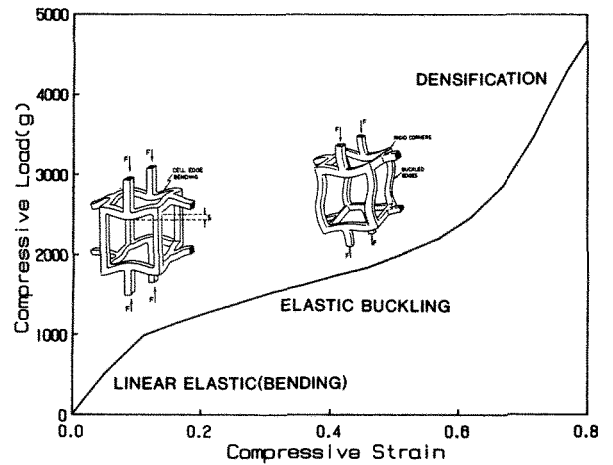


Figure 17 Compressive load-strain behavior for foam F3. (Insert drawings of model structures are from Ref. 16.)

in Figure 17 using the response for F3. Generally speaking, the shape of the load-strain behavior for the other foams tested is very similar. As noted, a linear elastic region takes place up to an approximate 10% strain level—at which point elastic buckling of the struts is believed to begin—and continues up to 60–70% strain. In the last region, the cellular walls begin to densify near a 60% strain level. Other investigators of flexible polyurethane foams have also observed and attributed the different “regimes” for the compressive load-strain behavior to similar ranges of strain level as shown in Figure 16.^{21,22} Based on the nonlinear behavior observed in Figure 17, it is expected that the changes in the cellular textures with strain are likely to influence the viscoelastic behavior of the load and/or the thickness of the foam. Before addressing this point, the general load relaxation behavior is discussed. An example of this behavior is shown in Figure 18 for F4 at 30–50% RH and at a constant strain level of 65%. In attempt to quantify the relaxation rate of these materials, the load relaxation has also been plotted in the form of $\log \text{load}(t)$ versus $\log t$ in Figure 18(b). From the slope of this rather linear relationship, the rate of relaxation or the load decay rate is obtained. As discussed earlier, a similar power law fit has also been observed for the tensile stress relaxation data of these same foams. A similar fit of the data has also been reported by a few investigators of flexible polyurethane foams, polyurethane elastomers, and some other polymeric network materials.^{16–19}

By utilizing the above method of evaluation for the load relaxation data, the load decay rate as a function of strain level was obtained and is displayed

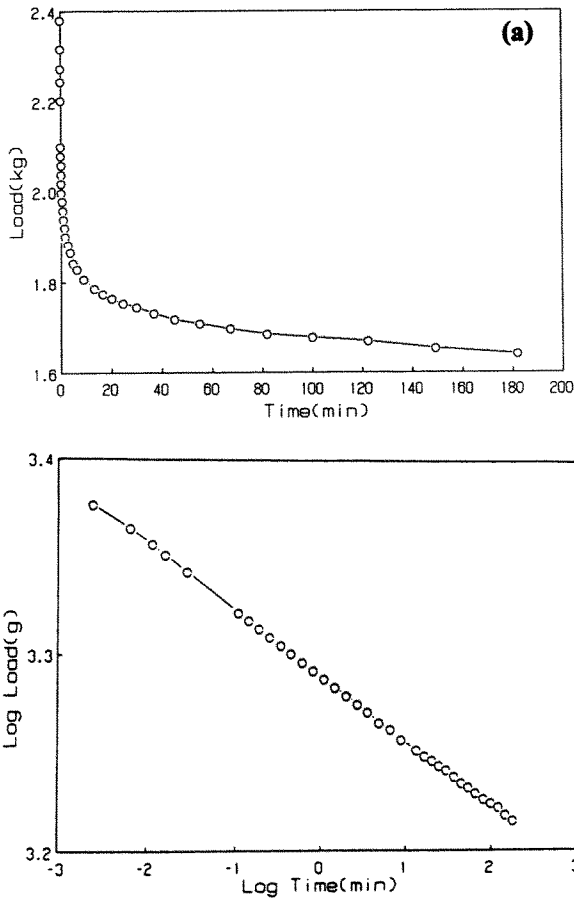


Figure 18 Compression load relaxation behavior at 30°C for foam F4 at a 65% strain level and 50% RH (a) linear load versus linear time and (b) log load versus log time.

in Figure 19 for Foam F3 at 30°C and 50% RH. As shown, the rate of relaxation is fairly constant up to a strain level of 65% or right at the verge of where densification is thought to begin to take place. At strains greater than 65%, the load decay rate increases and reaches a maximum near 75%. Similar behavior in this same region has also been observed for foams F1 and F4, but is not shown here.¹⁴ The increase in the rate of relaxation at the higher strain near 65% and greater is thought to be related to an intensification of the local strain of the cellular wall material. This local strain on the solid material is likely caused by the densification of the foam as exhibited in Figure 17 for the compressive load-strain curve. Based on the results shown in Figure 19 for the effect of strain level on the load decay rate and the common indentation load deflection (ILD) ASTM test used in testing flexible foams, the results presented in the paragraphs to follow were obtained

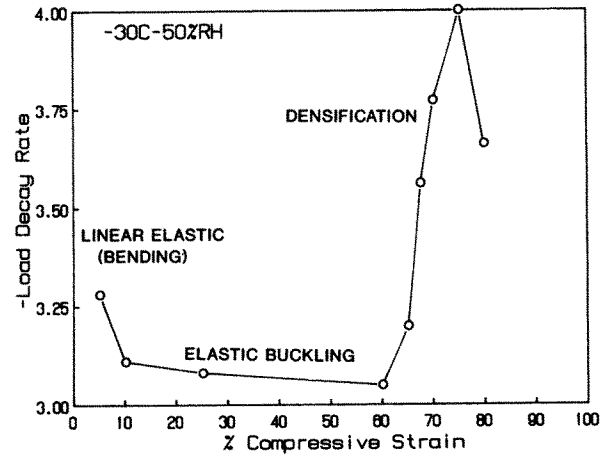


Figure 19 Effect of strain on load relaxation behavior for foam F3.

at an initial 65% strain level.¹³ The results that are discussed will consider the effects of temperature as well as humidity on the load relaxation behavior. Comparisons between results obtained in tension and compression are also made even though the strain levels were different and the behavior in the regimes of stress-strain curves are different.

The three-dimensional surfaces for the log load(*t*) – log *t* variable temperature compression load relaxation curves for foams F1 and F4 are presented in Figures 20 and 21, respectively. In addition, the initial load levels, the stress decay rates, and the percent load decay values at the different temperatures are summarized for F1 and F4 in Table VI. The initial load for F1 increases with temperature up to 100°C, whereas the initial load level for F4 changes very little with increasing temperature except for the decrease in this level near 85 to 100°C.

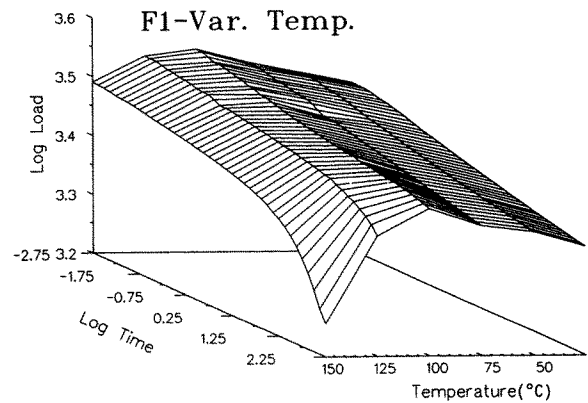


Figure 20 Log Load(*t*) – Log *t* variable temperature relaxation behavior for F1.

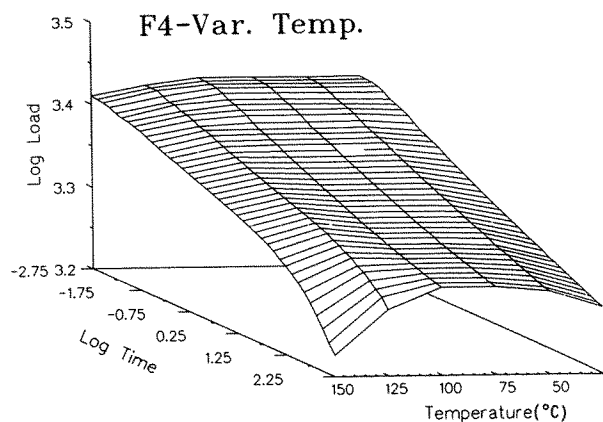


Figure 21 Log Load(t) – Log t variable temperature relaxation behavior for F4.

The 3-h load level for both foams behave similarly with increasing temperature as shown in Figures 22 and 23. As displayed in Figures 20 and 21 for F1 and F4, fairly linear behavior for the log load(t) versus log time over the 3-h testing period is exhibited up to temperatures of 100°C. In addition, the rate of relaxation and percent load decay values both decrease (even more so in F4) with increasing temperature in the range of 25 to 100°C (see Table III and Figure 21). This decrease in the amount of relaxation indicates, as suggested earlier for the tensile relaxation studies of these same foams, that the approach to an equilibrium load level appears to be accelerated with increasing temperature.

Based on the decrease in the relaxation rate with temperature, one might also speculate that additional cross-linking is taking place since these foams

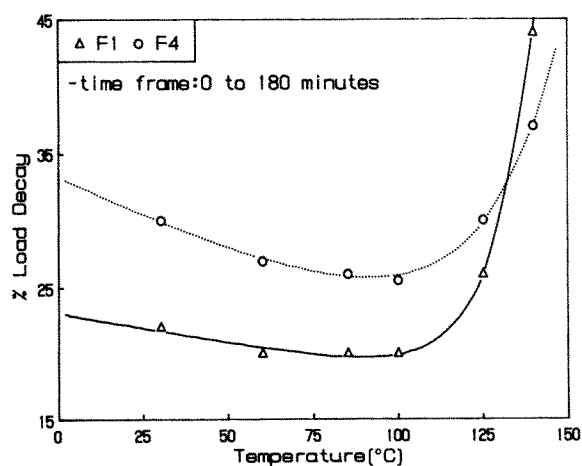


Figure 22 Compressive load decay at different temperatures for foams F1 and F4 (data points have been fitted by eq. (1)).

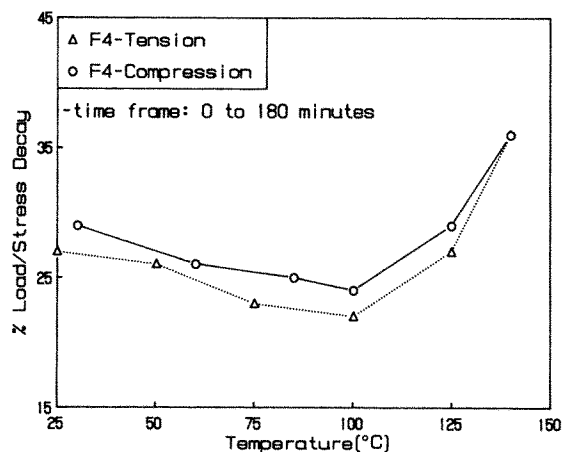


Figure 23 Comparison of percent decay values in tension and compression at different temperatures for foam F4.

are made with an excess of TDI. In determining if further cross-linking was occurring and, in turn, influencing the load relaxation response, the foams were thermally annealed at 100°C over short (3–4 h) and long (1 week) time periods. However, the effect of thermal annealing the foams at 100°C over both time periods had very little effect on the load relaxation behavior; thereby, giving further credibility to the data presented in Figures 20 and 21, that is, little decrease in either percent stress or load decay. Higher temperatures above 100°C, however, may well promote chemical changes with time as already discussed.

As shown in Figure 22 as well as in Table VI, there is a significant increase in the percent load

Table VI Summary of Results for Variable Temperature Compression Load Relaxation^a

Temperature (°C)	L_0 (kg) ^b		% Load Decay ^c		Slope ($\times 10^2$) ^d	
	F1	F4	F1	F4	F1	F4
30	3.1	2.7	22	30	-2.2	-3.2
60	3.2	2.7	20	27	-2.0	-2.9
85	3.3	2.7	20	26	-2.0	-2.7
100	3.5	2.7	20	26	-1.9	-2.6
125	3.4	2.6	26	30	-2.4	-2.8
140	3.1	2.6	44	37	-4.2	-3.6

^a The relative humidity was less than 1% for these data.

^b Initial load level obtained in ca. 0.2 sec following compression.

^c Time frame is from 0 to 180 min.

^d Slope is obtained by taking linear least squares of log load – log time data points; correlation coefficient is within 0.995–0.999 except at 125 and 140°C.

decay values for foams F1 and F4 at temperatures greater than 100°C. In addition, nonlinear behavior is observed in Figures 20 and 21 for both foams at temperatures greater than 100°C. As explained earlier for the variable temperature tensile stress relaxation behavior of these same foams, this significant increase in the amount of relaxation is attributed to an increase in the amount of hydrogen bonds that are being disrupted with increasing temperature as well as chain scission that is thought to take place within the urea and urethane linkages. Both of these changes in the microstructure of the foams have been indicated by FTIR thermal analysis of the plaques of these foams and will lead to further load decay.⁷ It is also important to note that some permanent set was observed at temperatures greater than 100°C and especially at 140°C for both foams.¹⁴ This observation gives further indication that some degradation is taking place at the higher temperatures.

In comparing Figure 22 (compression) with Figure 9 (tension), one will note that there are many striking similarities. First, the behavior of the percent load decay with temperature does fit the empirical model quite well given earlier in eq. [1] as demonstrated in Figure 21. The values for τ_1 and τ_2 obtained for the *compression load relaxation* behavior of foams F1 and F4 are comparable to those obtained from the *tensile stress relaxation* data, with the exception of τ_1 being somewhat different for the two modes for foam F1 (see Table VII). This difference is noticeable by the greater change in the stress decay values from 25 to 100°C in Figure 8 for F1 in comparison to the behavior in Figure 21. Also, the load decay values for F4 are higher than for F1 with the exception of the values at 140°C. As mentioned earlier, this difference is believed to be mostly related to F4 having the higher hard segment of the two foams and thus more available hydrogen bonds to undergo disruption. At 140°C, on the other hand, the reverse behavior is observed which is thought

to be related to degradation that occurs at temperatures greater than 100°C for both the urea and urethane linkages. As discussed earlier, the FTIR thermal analysis of the plaques of the foams suggested that chain scission is more significant in the lower hard-segment foam, F1, versus that of the higher, F4.⁷

The two response surfaces for F1 in compression (Fig. 20) and in tension (Fig. 6) are very comparable. In addition, the load or stress at a given time behaves similar with increasing temperature for the results obtained in tension and compression for F1. The surfaces for F4 in compression (Fig. 21) and tension (Fig. 7) are also similar with some differences in load and stress values at a given time with increasing temperature. In comparing the load decay values obtained in compression to the stress decay values in tension, results are shown as a function of temperature in Figure 23 for F4. It is noted here that the load decay values obtained in compression were adjusted slightly since the first data point was obtained on a shorter time scale in compression in comparison to that for the tensile studies. As shown in Figure 23, the values obtained in the two modes are comparable and thus suggests that the compression load relaxation behavior is rather independent of the cellular texture—the same conclusion that was drawn earlier for the tensile stress relaxation behavior of the foams!

Effect of Relative Humidity on Compression Load Relaxation Behavior

The log load-log t load relaxation behavior at 30 and 85°C from low to high humidity is shown for foams F1 and F4 in Figures 24 and 25, respectively. A summary of the load decay rates and the percent load decay values is given for both foams F1 and F4 in Table VII. As shown in Figures 24 and 25, the load level at a given time does decrease rather systematically with increasing relative humidity for

Table VII Constants for the Two-Parameter Model Describing the Thermal Dependence of Relaxation Behavior

Foam	$\tau_1(1/^\circ\text{C})$	C_1	$\tau_2(1/^\circ\text{C})$	C_2	$T_0(^\circ\text{C})$
Tension mode					
F1	258	60	14.9	1.19	373
F4	252	90	18.3	2.33	375
Compression mode					
F1	494	40	12.5	1.09	373
F4	272	90	21.5	3.71	375

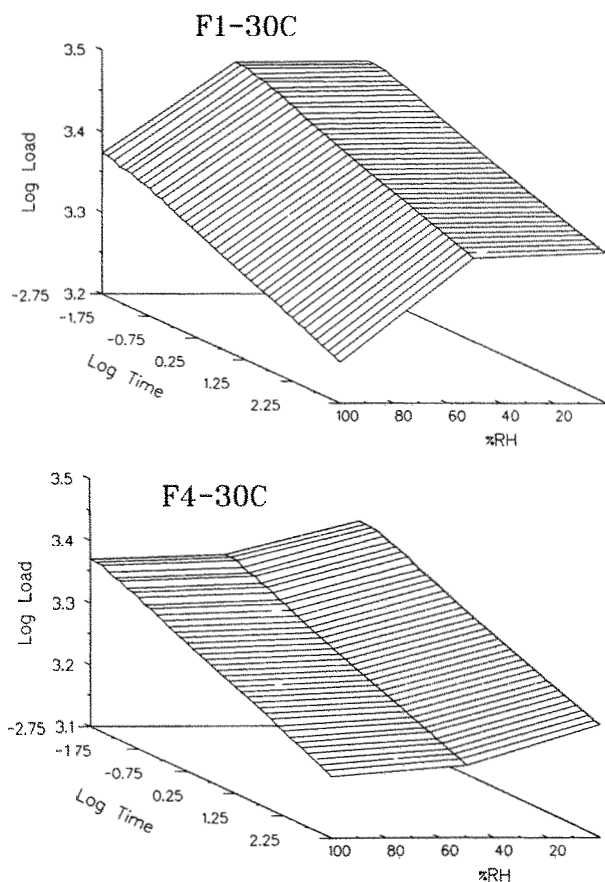


Figure 24 Effect of relative humidity on compression load relaxation behavior at 30°C for foams (a) F1 and (b) F4.

both foams at 30 and 85°C. As suggested earlier in the tensile relaxation studies, this decrease is attributed to water acting as a plasticizing agent.

At 30°C, the relaxation behavior for the 3-h testing period is near linear for log load of both foams F1 and F4 as exemplified by the results in Figure 24. In comparing the results of F1 with F4 (at 30°C), the percentage change in the relaxation behavior is slightly greater for F1 as shown by the results given in Table VII. At 60°C, however, the percentage change in the rates of decay are the same for F1 and F4. The results obtained at 30°C, therefore, imply that water interacts more with F1 in comparison to F4, whereas at 60°C, this interaction is similar for the two foams. This trend in the results at 30 and 60°C is comparable to the results obtained for the tensile stress relaxation behavior. One will also note that the rates of relaxation and the decay values in tension and compression are similar upon comparing the results in Tables V and VII, respectively. In ad-

dition, the response surfaces are rather comparable (compare Figure 12 with 23).

As shown in Figure 25 at 85°C for both foams, the relaxation behavior is also rather linear for the log load (t) for the 3-h time period, except for a small deviation from linearity at 85°C–95% RH. At 85°C, the percentage change in the relaxation behavior is greater for F4 than F1 which suggests the influence of water is greater for F4 at the higher temperatures. Again, this is believed to be related to the greater ability of water to interact with the hard segments due to a weakening of hydrogen bonds in the hard domains with increasing temperature. In comparing the results in tension and compression at the higher temperature, one will observe a comparable trend for the change in relaxation rates for F1 and F4 as well as similar relaxation behavior (see Tables V and VII, and Figures 14 and 25). The only exception to this last statement is the significant difference in the amount of relaxation observed at 85°C–95% RH in compression to that in tension at 90°C–95% RH for F4.

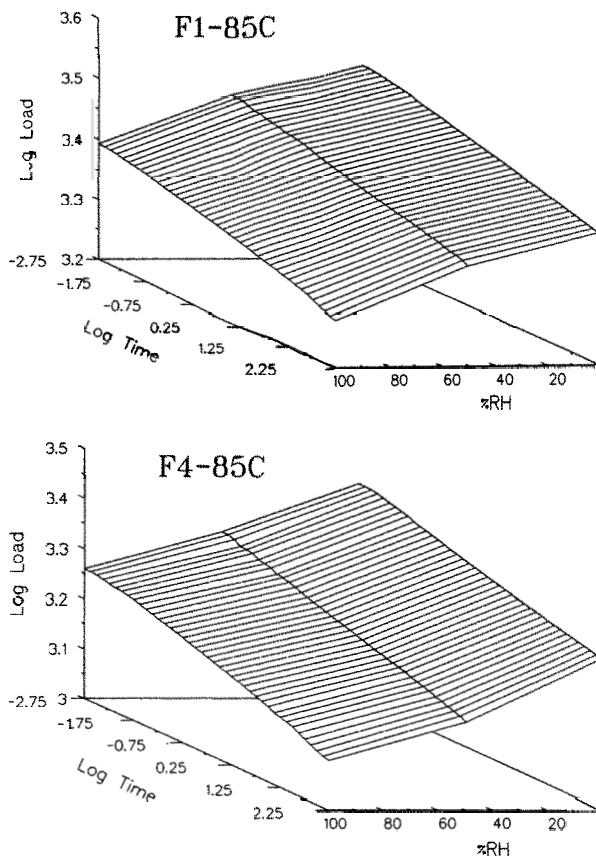


Figure 25 Effect of relative humidity on compression load relaxation behavior at 85°C for foams (a) F1 and (b) F4.

Table VIII Compression Load Relaxation Behavior at Different Temperature/Humidity Conditions

Foam	Temperature (°C)	% RH =	% Load Decay ^a (-Load Decay Rate × 10 ⁻²) ^b		
			0-15	50	95-100
F1	30		22 (2.2)	22 (2.3)	25 (2.6)
F4	30		30 (3.2)	31 (3.3)	33 (3.6)
F1	60		20 (2.0)	21 (2.1)	25.5 (2.5)
F4	60		28 (2.8)	30 (3.25)	32 (3.5)
F1	85		20 (2.0)	22 (2.2)	24 (2.4)
F4	85		26 (2.7)	30 (3.1)	32 (3.5)

^a Time frame is from 0 to 180 min for load decay values.

^b Correlation coefficient is within 0.995-0.999, except at 85°C-95% RH.

Overall, many similarities are observed in the compression and tension deformation modes, even though the constant level of strain utilized was higher in compression. Although there are some differences in the relaxation behavior, the resemblance exemplified by the corresponding response surfaces and furthermore by the comparable load and stress decay rates as well as the load and stress decay values are much more noteworthy than these differences. It is also important to recall that the studies in tension revealed that the stress relaxation behavior for the foams is governed by the solid portion of the foam. Thus, based on the many similarities in the relaxation behavior in tension and compression as well as the conclusions drawn for the results in tension, it is believed that the relaxation behavior in compression (*at 65% strain*) is rather independent of the cellular texture of the foams used in these systems. This latter statement may not necessarily be valid, however, for other cellular structures.

CONCLUDING REMARKS

The stress relaxation behavior in tension at 25% elongation for flexible slabstock polyurethane foams is dependent on the solid portion of the foam and thus independent of its cellular texture. This conclusion is not only supported by the similar rates of relaxation obtained by stretching the foams parallel and perpendicular to the blow axis, but also by the similar thermal dependence on stress decay for foams F1 and F4 and their respective plaques. For compressive strain levels up to 65%, the compression load relaxation behavior for slabstock foams is rather independent of the cellular texture of the foam. This conclusion is based on the similar relax-

ation behavior in compression and tension for foams F1 and F4 and the conclusion drawn above for the tensile stress relaxation behavior concerning its dependence on the solid portion of the foam.

Temperature as well as relative humidity have similar effects on the tensile stress relaxation and compression load relaxation for flexible slabstock foams. By increasing temperature in the range of 25-100°C, the viscoelastic decay, that is, tensile stress relaxation and compression load relaxation over 3 h is accelerated. This conclusion is based on the observance of a small decrease in the 3-h relaxation rates in tension and compression. For both viscoelastic tests, a significant increase in the viscoelastic decay at temperatures greater than 100°C is observed. This increase is attributed to additional mechanisms for relaxation and creep that are believed mostly related to hydrogen bond disruption in the hard segment regions and degradation of urea and urethane linkages. Within the temperature range of 25-125°C, higher rates of relaxation as well as a greater amount of relaxation is observed for the higher hard-segment foam due mostly to its higher hydrogen bonding content. At temperatures greater than 125°C, a larger amount of relaxation is observed for foam F1. This change in behavior is believed to be due to the lower structural order in foam F1 in comparison to F4. Increasing relative humidity at a given temperature does cause an increase in the viscoelastic decay as well as a decrease in the load of flexible foams. Such changes are believed to be due to water acting as a plasticizer and thus promoting localized chain slippage to take place. The effects of relative humidity on the tensile stress relaxation and compression load relaxation are greater on foam F1, than that of foam F4 at the lower temperatures and more significant on F4 at the higher

temperatures. This difference in behavior is believed to be due to water interacting more with the hard domains with increasing temperature. In comparing the effects of temperature and relative humidity on the viscoelastic decay as described by stress relaxation, compression load relaxation, and compression creep, temperature does have a greater effect than humidity on the relaxation behavior of flexible slab-stock polyurethane foams. In adding to the understanding of the viscoelastic behavior of flexible polyurethane foams, results obtained for the compressive creep behavior of foams F1 and F4 will be presented in a later paper.

G.L.W. and J.C.M. would like to thank Dow Chemical for financial support of this research and preparation of the well-defined foam samples. A special thanks goes to Bob Kuklies of Dow Chemical for his efforts in preparing the foam samples for the compression load relaxation studies.

REFERENCES

1. W. Patten and C. G. Seefried, *J. Cell. Plastics*, **12**, 41 (1976).
2. R. M. Herrington and D. L. Klarfeld, *Proc. of the SPI-6th International Tech./Marketing Conf.*, **177** (1983).
3. K. Saotome, K. Maturbara, and T. Yatomi, *J. Cell. Plastics*, **13**, 203 (1977).
4. J. M. Hogan, C. J. Person, T. H. Rogers, and J. R. White, *J. Cell. Plastics*, **9**, 221 (1973).
5. W. Patten and D. C. Priest, *J. Cell. Plastics*, **8**, 134 (1972).
6. R. P. Kane, *J. Cell. Plastics*, **7**, 5 (1971).
7. W. Patten, C. G. Seefried, R. D. Whitman, and D. E. Pollart, *J. Cell. Plastics*, **10**, 172 (1972).
8. R. B. Turner, H. L. Spell, and G. L. Wilkes, *SPI 28th Annual Technical/Marketing Conference*, **244** (1984).
9. J. P. Armistead, G. L. Wilkes, and R. B. Turner, *J. Appl. Polym. Sci.*, **35**, 601 (1988).
10. J. C. Moreland, G. L. Wilkes, and R. B. Turner, *J. Appl. Polym. Sci.*, **43**, 801 (1991).
11. W. M. Lee, *Proc. of the SPI-30th Annual Tech./Marketing Conf.*, **138** (1985).
12. F. J. Dywer, *J. Cell. Plastics*, **12**, 104 (1976).
13. ASTM Standards, D3574 **9**(2), (1986).
14. J. C. Moreland, Ph.D. Thesis, Virginia Polytechnic Institute and State University, Chemical Engineering Dept., Blackburg, VA, 1991.
15. N. C. Hilyard, *Mechanics of Cellular Solids*, Applied Sci. Publishers, LTD, New Jersey, 1980.
16. M. F. Ashby, *Mettallurgical Trans*, **14A**, 1755 (1983).
17. J. C. Moreland, Masters Thesis, Virginia Polytechnic Institute and State University, Chemical Engineering Dept., Blackburg, VA, 1989.
18. C. S. Paik Sung, C. B. Hu, and C. S. Wu, *Macromol.*, **13**, 111 (1980).
19. T. L. Smith and R. A. Dickie, *J. Polym. Sci., Part A-2*, **7**, 635 (1969).
20. D. J. Doherty and G. W. Ball, *J. Cell Plastics*, **3**(5), (1967).
21. E. A. Meincke and R. C. Clark, *The Mechanical Properties of Polymeric Foams*, Technomic Publishing Co., Inc., Westport, Conn., 1973.
22. R. W. Seymour, G. M. Estes, D. S. Huh, and S. L. Cooper, *J. Polym. Sci.*, **10**(A-2), 1521 (1972).

Received September 14, 1992

Accepted October 18, 1993